Nat. Hazards Earth Syst. Sci. Discuss., 3, 6947–6976, 2015
www.nat-hazards-earth-syst-sci-discuss.net/3/6947/2015/
doi:10.5194/nhessd-3-6947-2015

Natural Hazards and Earth System Sciences
Open Access
Discussions

Evaluation of the initial stage of the reactivated Cotopaxi volcano – analysis of the first ejected fine-grained material

T. Toulkeridis[1,4], C. R. Arroyo[2], M. Cruz D'Howitt[3], A. Debut[2], A. V. Vaca[2], L. Cumbal[2], F. Mato[1], and E. Aguilera[3]

[1]Departamento de Seguridad y Defensa, Universidad de las Fuerzas Armadas ESPE, P.O. Box 171-5-231, Sangolquí, Ecuador
[2]Centro de Nanociencia y Nanotecnología, Universidad de las Fuerzas Armadas ESPE, P.O. Box 171-5-231B, Sangolquí, Ecuador
[3]Departamento de Ciencias de la Tierra y Construcción, Universidad de las Fuerzas Armadas ESPE, P.O. Box 171-5-231, Sangolquí, Ecuador
[4]Centro Panamericano de Estudios e Investigaciones Geográficas (CEPEIGE), Quito, Ecuador

Received: 14 October 2015 – Accepted: 30 October 2015 – Published: 18 November 2015

Correspondence to: T. Toulkeridis (ttoulkeridis@espe.edu.ec)
and C. R. Arroyo (ccarroyo@espe.edu.ec)

Published by Copernicus Publications on behalf of the European Geosciences Union.

Abstract

Fine-grained volcanic samples were collected at different locations near the Cotopaxi volcano on the same day of its reactivation and some days afterwards in August 2015. The wind-directions charged with such materials have been determined and compared with the existing data-base allowing preventive measures about local warning. The obtained data yielded the less expected wind-directions and therefore ash precipitation in usually less affected areas towards the northern and eastern side of Cotopaxi volcano. The collected samples were studied basically for their morphology, content in minerals and rock fragments as well as the chemical composition. The results obtained from this study allowed to identify and classify the origin of the expelled material being hydroclasts of andesites and dacites with rare appearances of rhyodacites and associated regular as well as accessory minerals all being present in the conduct and crater forming part of previous eruptive activities of the volcano. A further evaluation has been performed to determine the activity stage of the volcanic behavior. The resulting interpretation appears to point to a volcanic behavior a more frequent sporadic event with a relatively low probability of lahar generation rather than any other known destructive phase, which includes a less-frequent but tremendously more catastrophic scenario.

1 Introduction

Volcanoes and associated hazards have been responsible for the death of hundreds of thousands of persons in the last two centuries worldwide (Peterson, 1988; Tanguy et al., 1998). They destroyed a variety of strategic infrastructure throughout the world, changed the local and global climate (Hofmann and Rosen, 1983; Self and Rampino, 1988; Pinatubo Volcano Observatory Team, 1991; Hansen et al., 1992; Briffa et al., 1998) as well as nearby landscapes (Blong, 1984; Jago and Boyd, 2005; Scott et al., 2010). Expelled pyroclastic material such as ash, pumice and bombs are one of the most underestimated yet most hazardous volcanic phenomena (Miller and Casadevall,

1999; Self, 2006; Barsotti et al., 2010; Dingwell and Rutgersson, 2014). Nonetheless, one of the most lethal volcanic hazards are lahars, as they are more devastating in terms of cumulative fatalities than all other volcanic hazards including pyroclastic flows (Sigurdsson and Carey, 1986; Rodolfo, 1999).

Cotopaxi volcano in the northern volcanic Andes is known to have had a vast history of lahar generations (Barberi et al., 1995; Aguilera et al., 2004; Aguilera and Toulkeridis, 2005; Pistolesi, 2008; Pistolesi et al., 2013, 2014). As the volcano awakens, it is fundamental to prove its behavior and potential of generating big eruptions and subsequent lahars similar and worse related to the disaster in Armero Colombia in 1985 (Naranjo et al., 1986; Thouret, 1990; Pierson et al., 1990). In order to accomplish the evaluation of the stage if volcanic activity we have taken samples of the very first expelled fine-grained material with the goal to determine if the reactivation of Cotopaxi volcano is more likely minor sporadic event or the initial stage of a severe eruptive event (Heiken, 1972; Houghton and Smith, 1993; Büttner et al., 1999; Dellino and Liotino, 2002).

2 Geodynamic background, volcanic history and sample location

The northern Andes in Ecuador are part of the 7000 km long classic example of an active continental margin along the South American continent, with several volcanic sequences of Mesozoic and Cenozoic ages. More than 250 volcanoes are exposed in the Ecuadorian part of the Northern Andean Volcanic Zone (NAVZ) of which the 5897 m a.s.l. high Cotopaxi, is one of the twenty considered active volcanoes in the country as result of the subduction of the oceanic Nazca plate below the South American continent (Lonsdale, 1978; Barberi et al., 1988; Freymuller et al., 1993; Toulkeridis, 2013). In the area of Ecuador, the Nazca Pacific plate is subducted at an angle slightly oblique to the southern American continent, producing an overall active tectonic regime with transpression due to its convergence. The consequences of this subduction are four morphologically distinctive volcanic chains (Toulkeridis, 2013; Fig. 1).

The Cotopaxi stratovolcano in Ecuador, which has been formed in the Pleistocene, is located some 60 km south of Quito and represents a natural laboratory for the assessment of volcanic hazards. The current volcano consists of two craters, one older and one more recent. The more recently created crater is snow-covered and is the site of volcanic vent activity. The magmatic activity of the volcano in historical times is well documented (La Condamine, 1751; von Humboldt, 1837, 1838; Reiss, 1874; Sodiro, 1877; Stübel, 1897; Whymper, 1892; Wolf, 1878, 1904; Reiss and Stübel, 1869–1902; Barberi et al., 1995) and the lahars produced by the volcano have affected considerably the villages, cities and infrastructure in its surroundings. Some 19 eruptive phases have been registered and dated giving a re-occurrence of its activity every 117 ± 70 years over the last 2200 years (Barberi et al., 1995; Aguilera and Toulkeridis, 2005). The last four volcanic phases with the generation of lahars and subsequent destruction of nearby villages occurred in 1534, 1742, 1768 and 1877 (Barberi et al., 1995; Aguilera and Toulkeridis, 2005). At least one partial sector collapse takes also part of Cotopaxi's development some 4600 years ago, leading to a major debris avalanche (Mothes et al., 1998) covering most of the past northern drainages.

The best-documented event took place in 1877 and ended up killing approximately 1000 people in the area (Sodiro, 1877). Glacier melting facilitated the creation of a lahar, which roared down the mountain at speeds of up to 70 km h^{-1} (Aguilera et al., 2004). Although the glacier is currently retreating, circumstances have much changed since the 1877 lahar. Thus although a future lahar would be smaller than that of 1877, the fact that many more people are living within the area suggests that the loss of life could be much higher than in the past. Whereas about 30 000 people were living in the danger area in the late 1800s, currently the number is greater than 500 000. The most dangerous areas would be the South, East, and North sides due to flow patterns. Unfortunately the nearest cities would be hit within 30 min from the formation of a lahar, with little warning for evacuation (Aguilera et al., 2004; Aguilera and Toulkeridis, 2005). In addition to these highly destructive volcanic events, similar to 1877, some additional 59 other explosions have been recorded between 1532 and 2015, 27

of which included lava flows and/or minor lahars (Barberi et al., 2005; Aguilera et al., 2004; Aguilera and Toulkeridis, 2005). Based on statistical data from the last 19 eruptive phases over 2200 years, the probability of a new occurrence in the year 2015 is of about 72 %, while the re-occurrence of a minor volcanic event, like the 59 sporadic explosions is much higher.

By the end of 2001, after decades without visible activity, Cotopaxi has shown signs of unrest with some increasing seismic activity, gas from a variety of fumaroles and the main crater and also small phreatic explosions (Toulkeridis and Aguilera, 2003, 2004; Cerca et al., 2005a, b; Toulkeridis, 2006, 2007a, b, 2010, 2012). The evaluation of such volcanic signs is fundamental in order to characterize and determine the next volcanic event, as it may include a volcanic phase with the subsequent generation of lahars or a minor event similar to the almost sixty reported ones. The newly seismic and volcanic gas activity of Cotopaxi showed ups and downs, having a peak activity since April 2015. Seismic signs reached up to a few hundreds per day, while emissions of SO_2 reached up to 5000 t a day (IG-EPN, 2015).

After the highest registered seismic activity in months at 17:27 ECT (Ecuador time) in the night of the 13 August, a clear precursor of an imminent explosion took place. In the morning of the 14 August at 04:02 and 04:07 ECT (Fig. 2) the very first two explosions occurred, followed by three more at 10:25 ECT (Fig. 3), 13:45 and 14:29 ECT. The fine-grained material has been distributed towards north-northwest and to the east. Sample collection has been performed at 5400 m a.s.l. at the northern side of Cotopaxi volcano during the first explosions at 04:00 ECT in the morning (sample COT-1408-4), close to Machachi (COT-1408-3), at Cotogchoa-Amaguaña (COT-1408-2) and ESPE campus (COT-1408-1; Fig. 2).

3 Analytical procedures

We have used available data from the Ecuador Satellite Imagery of the Satellite Services Division of the National Environmental Satellite, Data, and Information Service

(NESDIS) for the period between September 1999 and September 2015. Some 4799 images were evaluated for their wind direction and were weighted for the main direction of the ash charged cloud and their respective flanks (Toulkeridis and Zach, 2015). A total of 19 196 data of the 4799 images were subdivided per month in order to determine the main wind directions for the different seasons in Ecuador. Around 90.29 % of the obtained data belongs to Tungurahua volcano, 4.04 % to El Reventador volcano, 2.63 % to Sangay volcano, 2.40 % to Cotopaxi volcano and the remaining 0.65 % to Guagua Pichincha volcano. The altitude of the ash clouds is varying between FL180 and FL400, with two predominant heights being between FL200 and FL250 and a further between FL 300 and FL400, generating together some 98 % of all available data. This data set has been plotted in regular rose diagrams and it provides an excellent overview on the wind directions of ash clouds of representative active volcanoes in the Ecuadorian mainland compared with the actual data provides by the reactivation of Cotopaxi volcano (Fig. 4).

Volcanic fine-grained material collection has been achieved by either metal or teflon-like plastic funnels leading to a metallic tray and from there the material has been taken and sealed for further analysis into sample beakers. The sites of the collection were chosen to be implemented in areas with the highest probability of ash precipitation as known by the evaluation of the wind directions of ash-charged clouds for the years 1999 up to 2015 (Toulkeridis and Zach, 2015; Fig. 4). For the characterization, evaluation and analysis of all pyroclastic samples, we have used a portable optical microscope, field emission gun scanning electron microscope (FEG-SEM) equipped with an energy dispersive spectrometer (EDS) and additionally we have also used an X-ray diffraction (XRD) setup.

All samples where firstly analyzed with Celestron (model 44302-A) portable optical microscope with an amplification capacity of 10X to 150X, giving the opportunity to realize micrometric determinations down to 0.01 mm in size (Fig. 5).

The SEM inspection was performed using a TESCAN MIRA3. The fine-grained samples were fixed onto SEM stubs using an adhesive layer and sputter-coated with gold

(99.99 % purity) before the SEM imaging. SEM images at different magnification (150X and 8000X) were taken with a resolution of 1024 × 917 pixels (Figs. 6 and 7, respectively).

The chemical analysis was carried out by an EDS of the brand BRUKER model Quantax 200, installed in the SEM chamber and a detector XFlash 6130, reaching a resolution of 124 eV.

XRD studies were carried out using a PANalytical EMPYREAN setup within a 2θ configuration (generator-detector) x-ray tube copper λ = 1.54 Å and XCELERATOR detector (minimum angle step 0.0001°). To perform the measurements shown in this work, the ash powder samples were directly deposited on optical microscope slides. The mineral composition of the samples was determined by using the PAN-ICDS database.

4 Results and discussion

4.1 The main event

Seismographs of the Instituto Geofísico of the Escuela Politécnica Nacional (IG-EPN) registered seismic unrest in the evening prior to the main explosion of the early morning of the 14 August (IG-EPN, 2015). Such kind of precursors have been registered in Ecuador various times without any warning or indication of the IG-EPN towards authorities or public, such like the seismic events of Reventador volcano with its eruption (VEI = 4) on 3 November 2002, of Sierra Negra volcano on 22 October 2005 (VEI = 3), of Tungurahua volcano with a following destructive eruption (VEI = 3) on 14 July and 17 August 2006, and Wolf volcano in June 2015 (Monzier et al., 1999; Garcia-Aristizabal et al., 2007; Toulkeridis et al., 2007; Arellano et al., 2008; Barrancos et al., 2008; Carn et al., 2008; Hall et al., 2008; Ridolfi et al., 2008; Robin et al., 2008; Lees et al., 2008; Steffke et al., 2010; McCormick et al., 2014; Smithsonian Institute, 2015). Therefore, the non-warning of such precursor did not really surprise. At 04:02 and 04:07 ECT of the 14 August an eight km high eruption column of a phreatic

explosion took place associated with a shaking of the volcano as felt by professional climbers at the moment of the emplacement as well as some rock falls and glacial fragmentation as seen by the same persons and accompanying tourists. Besides ash, some smaller rock fragments of andesites and dacites reached to an altitude of approximately 5400 m a.s.l., the coarsest being 4 cm in size. Later eruptions in the same morning and afternoon have been reported and being visible to authorities and public alike. As result of the visibility of later eruptions and their respective eruptive columns of up to 5 km in altitude forced the Ecuadorian Secretary of Risk Management (Secretaría de Gestión de Riesgos; SGR) to change the alert status from white into yellow, meaning seven hours after the main event. Therefore it can be concluded, that the change of the alert status of the Cotopaxi volcano occurred due to the visibility of the explosive event of 10:25 ECT (Fig. 3) and not through any merits of monitoring or instrumental data analysis.

4.2 Wind directions

Wind directions of ash-charged clouds are relatively uniform from E to W from April to September and varies and changes slightly into E-W, E-NE to W-SW but also to other less frequent directions such as W–E and SE-NW. Therefore, the period between April and September is the best predictable one, while the rest of the year has a relatively high probability to present the same direction with some variation of lesser extent. As the data set is based on the past volcanic activity of four volcanoes, these volcanoes namely Tungurahua, Guagua Pichincha and Reventador, but not Sangay, were responsible for a variety of route changes of airplanes and the closure of airport activities (Smithsonian Institute, 2015). Nonetheless, comparing the available data set (Toulkeridis and Zach, 2015) with the actual behavior of the ash-charged clouds of the 14 August event of Cotopaxi volcano, one of the most unlikely and less probable wind directions took place, namely towards the E and NNW. Later events, of the following days shifted towards most probable and expected wind directions being E to W and NE

to SW (Fig. 4). Therefore later fine-grained samples where taken in Lasso being along the main, predominant wind direction.

4.3 Characterization of the sampled particles

The preliminary visual inspection of the fine-grained samples performed with an optical microscope determined an association of particles of which rims have exclusively angular shapes and acute edges with sizes between 0.70 to 0.01 mm. The finest particles of COT-1408-3 making up some 20 % of the sample are between 0.01 to 0.07 mm in size, while the majority (70 %) has a size between 0.12 to 0.17 mm. Some coarser rock fragments have been identified with sizes between 0.5 to 0.7 mm (Fig. 5).

The characterized material is represented by rock fragments of porphyritic andesites and some minor dacites with the rarely presence of rhyodacites, all being hydroclasts (Schmincke, 2004), while the lose minerals contained quartz, mica, hornblendes, plagioclases (mainly anorthites), volcanic glass (obsidian), pyrites and also galena besides other accessory minerals. While almost all material recognized are most likely associated with typical volcanic material provided by the conduct and crater of Cotopaxi volcano, the galena may have been formed by some recent hydrothermal activity in the volcano or may have been part of the underlying metamorphic basement and brought up by the volcanic activity.

The angular shape of the rock fragments as well as their minerals, the nonexistence of newly formed (juvenile) magmatic material evidences an exclusively hydrothermal explosive origin (Figs. 6 and 7). The size fractions of the analyzed material of the ESPE campus being some 60 km in distance of the volcano, together with the known explosion height of 8 km, suggests a violent explosion. This explosion most probably liberated over-pressured water vapor originated of over-heated subterranean infiltrated water, which fragmented and hydrothermalized rocks, minerals and pre-existing ash of the volcanic conduct and some fissured of the crater.

Table 1 illustrates the chemical analysis from COT-1408-1, COT-1408-2, COT-1408-3 and COT-1408-4 obtained by EDS measurements. To take into account the inhomo-

geneity of the samples, we have averaged the spectra obtained from 100 points grid on a total area of 1.96 mm^2. The presence of each element is denoted by the normalized weight percentage (norm. w.t. %), which is the percentage in weight, supposing that the elements in the table represent total composition of the sample. For clarity we have neglected the presence of oxygen and carbon, which are present in great abundance (higher than 50 %). The margin of error corresponds to the 68 % confidence interval. The samples rich in sulfur, were taken close to the volcano, while the ones having high contents in iron, magnesium, manganese were located far away. Iron appeared on samples far away from volcano because most likely they were oxidized with atmospheric oxygen and falls down as a Fe(III) precipitate as soon as it gets denser particle. The biggest difference of COT-1408-4 as compared to COT-1408-1, COT-1408-2 and COT-1408-3 is the high concentration of sulfur.

The standard 2θ configuration in the XRD setup was used to analyze the mineral composition of all samples. The four samples show quite similar spectra and the analysis reveals composition of a typical Na-rich Anorthite. The slight differences observed in the main peaks from one sample to another are due to the non-inhomogeneity and granularity of the samples.

4.4 Granulometry

As previously mentioned four samples of the very first eruption event on 14 August located at different sites but within the precipitation area of the northern side of the ash-charged cloud were collected, representing a unique data set.

Figure 6a–d shows representative SEM micrographs (150X) obtained from the samples where the size distribution and the morphology of the particles can be observed. Using the MIRA3 SEM software we have calculated the size distribution of the particles from manual diameter determination over a minimum of 100 particles for each sample. In Fig. 8a–d we illustrate the diameter particle histograms obtained from the analysis of the samples. A careful inspection of the particle surface reveals the existence of even

smaller particles (see Fig. 7). The mean values, standard deviations and confidence intervals obtained for all samples are summarized in the Table 2.

The samples show different size distribution being coarser at Machachi close to the Cotopaxi Volcano. Sample COT-1408-3 shows unusually two different peaks at the particle diameter histogram (Fig. 8c). Nonetheless, the finer first peak at around 100 µm and may be correlated to the peak observed on sample COT-1408-1 and COT-1408-2. Although the particles have all the same origin they clearly have different surface structures for each sample (Fig. 7). Particles may get oxidized or undergo different erosion patterns due to changes of wind direction.

Later events after the 22 August (sample COT-2208-1) have similar rough surfaces, with apparently identical angular rims of rock fragments and minerals, while the mineral-size distribution is evidently reduced in Lasso and Machachi samples (Table 3; Figs. 9 and 10).

5 Conclusions

The chemical and morphological evaluation of different fine-grained samples of the very first ejected material collected in the vicinity of the Cotopaxi volcano, after decades of tranquility, was able to determine the activity stage and potential magma behavior.

The ash-charged wind directions have been unusual for this time of the year compared to averaged data set collected during 15 years. Nonetheless, the initial explosions directed towards the NNW and E changed shortly afterwards and remained stable being W–E and WNW–ESE reaching even coastal areas.

The shape of the rock fragments and minerals expelled on the first eruptive event in the early morning of the 14 August as well as pyroclastic material of later ejections have been exclusively characterized as fragmented and angular shaped. Juvenile magma at the proximity of the crater can therefore categorically be excluded.

The mineral classification and also the chemical composition of the ejected material determined a typical andesitic to dacitic and rarely rhyodacitic composition with a high

abundance of classical mineral composition of such rocks, being plagioclases, quartz, biotite, hornblende but also obsidian, pyrite and some other accessory minerals.

The size distribution of the expelled pyroclastic material has been continuously reduced, most probably due to the decreasing intensity of the volcanic pulses with time, evidently in the Machachi and Lasso samples on the W and SW edge of the volcano.

Additionally it can be concluded, that the volcanic activity stage of Cotopaxi volcano represents clearly a frequent minor sporadic event rather than a less occurring severe eruptive event. Therefore major explosions and the generation of far-reaching lahars is excluded for the time such volcanic activity is present.

Knowing the composition and morphology of the fine-grained particles in almost real-time can be considered as a great information for understanding the mechanisms underlying the reactivation process of volcanoes. Finally, this should be used in the future by the authorities for making decisions in order to avoid public awareness and uncertainties.

Acknowledgements. Carlos R. Arroyo and Fernando Mato acknowledge support from the Prometeo Project of the National Secretariat of Higher Education, Science, Technology and Innovation (SENESCYT), Ecuador. We are thankful for receiving samples by Veronica Rubio, Fernando Tovar, Julian Lara and Jendri Pazmiño (Tovar Expeditions; crater), Alexandra Ayala (Machachi), Oswaldo Padilla (Cotogchoa), Mario Cruz (ESPE) as well as Carlos Zaldumbide, Santiago Tapia and Rocio Herrera (Novacero and Provefrut; Lasso).

References

Aguilera, E., Pareschi, M. T., Rosi, M., and Zanchetta, G.: Risk from lahars in the northern valleys of Cotopaxi Volcano (Ecuador), Nat. Hazards, 33, 161–189, 2004.

Arellano, S. R., Hall, M., Samaniego, P., Ruiz, A., Molina, I., Palacios, P., Yepes, H., and OVTIGEPN staff: Degassing patterns of Tungurahua volcano (Ecuador) during the 1999–2006 eruptive period, inferred from remote spectroscopic measurements of SO_2 emissions, J. Volcanol. Geoth. Res., 176, 151–162, 2008.

Barberi, F., Coltelli, M., Ferrara, G., Innocenti, F., Navarro, J. M., and Santacroce, R.: Plio-quaternary volcanism in Ecuador, Geol. Mag., 125, 1–14, 1988.
Barberi, F., Coltelli, M., Frullani, A., Rosi, M., and Almeida, E.: Chronology and dispersal characteristics of recently (last 5000 years) erupted tephra of Cotopaxi (Ecuador): implications for long-term eruptive forecasting, J. Volcanol. Geoth. Res., 69, 217–239, 1995.
Barrancos, J., Roselló, J. I., Calvo, D., Padrón, E., Melián, G., Hernández, P. A., M. Pérez, N., Millán M., and Galle, B.: SO_2 emission from active volcanoes measured simultaneously by COSPEC and mini-DOAS, Pure Appl. Geophys., 165, 115–133, 2008.
Barsotti, S., Andronico, D., Neri, A., Del Carlo, P., Baxter, P. J., Aspinall, W. P., and Hincks, T.: Quantitative assessment of volcanic ash hazards for health and infrastructure at Mt. Etna (Italy) by numerical simulation, J. Volcanol. Geoth. Res., 192, 85–96, 2010.
Blong, R. J.: Volcanic Hazards, Academic Press, Sydney, Australia, 424 pp., 1984.
Briffa, K. R., Jones, P. D., Schweingruber, F. H., and Osborn, T. J.: Influence of volcanic eruptions on Northern Hemisphere summer temperature over the past 600 years, Nature, 393, 450–455, 1998.
Büttner, R., Dellino, P., and Zimanowski, B.: Identifying magma–water interaction from the surface features of ash particles, Nature, 401, 688–690, 1999.
Carn, S. A., Krueger, A. J., Krotkov, N. A., Arellano, S., and Yang, K.: Daily monitoring of Ecuadorian volcanic degassing from space, J. Volcanol. Geoth. Res., 176, 141–150, 2008.
Cerca, M., Concha-Dimas, A., and Toulkeridis, T.: Structural Setting and Emplacement Model of the Cotopaxi Volcanic Complex, Ecuador: Preliminary Results, Reunion Annual de la Union Geofisica Mexicana, Puerta Vallarta, Mexico, 2005a.
Cerca, M., Toulkeridis, T., and Concha-Dimas, A.: First results about the structural setting and emplacement model of the Cotopaxi Volcanic Complex, Ecuador, Chapman Conference on the Effects of Basement, Structure, and Stratigraphic Heritages on Volcano Behaviour, Taal Volcano, Tagaytay City, Philippines, p. 36, 2005b.
Dellino, P. and Liotino, G.: The fractal and multifractal dimension of volcanic ash particles contour: a test study on the utility and volcanological relevance, J. Volcanol. Geoth. Res., 113, 1–18, 2002.
Dingwell, A. and Rutgersson, A.: Estimating volcanic ash hazard in European airspace, J. Volcanol. Geoth. Res., 286, 55–66, 2014.
Freymuller, J. T., Kellogg, J. N., and Vega, V.: Plate motions in the north Andean region, J. Geophys. Res., 98, 21853– 21863, 1993.

Garcia-Aristizabal, A., Kumagai, H., Samaniego, P., Mothes, P., Yepes, H., and Monzier, M.: Seismic, petrologic, and geodetic analyses of the 1999 dome-forming eruption of Guagua Pichincha volcano, Ecuador, J. Volcanol. Geoth. Res., 161, 333–351, 2007.
Hall, M. L., Samaniego, P., Le Pennec, J. L., and Johnson, J. B.: Ecuadorian Andes volcanism: a review of Late Pliocene to present activity, J. Volcanol. Geoth. Res., 176, 1–6, 2008.
Hansen, J., Lacis, A., Ruedy, R., and Sato, M.: Potential climate impact of Mount Pinatubo Eruption, Geophys. Res. Lett., 19, 215–218, 1992.
Heiken, G.: Morphology and petrography of volcanic ashes, Geol. Soc. Am. Bull., 83, 1961–1988, 1972.
Hofmann, D. J. and Rosen, J. M.: Sulfuric acid droplet formation and growth in the stratosphere after the 1982 eruption of El Chichon, Science, 222, 325–327, 1983.
Houghton, B. F. and Smith, R. T.: Recycling of magmatic clasts during explosive eruptions: estimating the true juvenile content of phreatomagmatic volcanic deposits, B. Volcanol., 55, 414–420, 1993.
IG-EPN: Reportes diarios de volcanes Ecuatorianos, Instituto Geofísico de la Escuela Politécnica Nacional, available at: http://www.igepn.edu.ec/informes-volcanicos/cotopaxi/coto-diarios/coto-d-2015 and http://www.igepn.edu.ec/informes-volcanicos/cotopaxi/coto-especiales/coto-e-2015, last access: November 2015.
Jago, L. C. and Boyd, W. E.: How a wet tropical rainforest copes with repeated volcanic destruction, Quaternary Res., 64, 399–406, 2005.
La Condamine Ch. Marie: Diario del Viaje al Ecuador, republ. in 1986, Quito, Publitécnica, Quito, 221 pp., 1751.
Lees, J. M., Johnson, J. B., Ruiz, M., Troncoso, L., and Welsh, M.: Reventador volcano 2005: eruptive activity inferred from seismo-acoustic observation, J. Volcanol. Geoth. Res., 176, 179–190, 2008.
Lonsdale, P.: Ecuadorian subduction system, AAPG Bull., 62, 2454– 2477, 1978.
McCormick, B. T., Herzog, M., Yiang, J., Edmonds, M., Mather, T. A. Carn, S. A. Hidalgo, S., and Langmann, B.: A comparison of satellite and ground based measurements of SO_2 emissions from Tungurahua volcano, Ecuador, J. Geophys. Res.-Atmos., 119, 4264–4285, 2014.
Meyer, H.: In den Hochanden von Ecuador, vols. Ix, Ixi, Ixii., Anal. Univ. Central., Quito, 1907.
Miller, T. P. and Casadevall, T. J.: Volcanic ash hazards to aviation, in: Encyclopedia of Volcanoes, edited by: Sigurdsson, H., Houghton, B., Rymer, H., Stix, J., and McNutt, S., Academic Press, 915–930, 1999.

Monzier, M., Robin, C., Samaniego, P., Hall, M. L., Cotten, J., Mothes, P., and Arnaud, N.: Sangay volcano, Ecuador: structural development, present activity and petrology, J. Volcanol. Geoth. Res., 90, 49–79, 1999.
Mothes, P., Hall, M., and Janda, R.: The Enormous Chillos Valley Lahar: an ash-flow generated debris flow from Cotopaxi volcano, Ecuador, B. Volcanol., 59, 233–244, 1998.
Naranjo, J. L., Sigurdsson, H., Carey, S. N., and Fritz, W.: Eruption of the Nevado del Ruiz volcano, Colombia, on 13 November 1985: tephra fall and lahars, Science, 233, 961–963, 1986.
Pierson, T. C., Janda, R. J., Thouret, J.-C., and Borrero, C. A.: Perturbation and melting of snow and ice by the 13 November 1985 eruption of Nevado del Ruiz, Colombia, and consequent mobilization, flow and deposition of lahars, J. Volcanol. Geoth. Res., 41, 17–66, 1990.
Pinatubo Volcano Observatory Team: Lessons from a major eruption: Mt. Pinatubo, Philippines, EOS T. Am. Geophys. Un., 72, 545–555, 1991.
Pistolesi, M.: Historical analysis and stratigraphy of the post-XII century pyroclastic activity at Cotopaxi volcano, Ecuador, Implication for lahar hazard assessment, Plinius, 34, 131–138, 2008.
Pistolesi, M., Cioni, R., Rosi, M., Cashman, K. V., Rossotti, A., and Aguilera, E.: Evidence for lahar-triggering mechanisms in complex stratigraphic sequences: the post-twelfth century eruptive activity of Cotopaxi Volcano, Ecuador. B. Volcanol., 75, 1–18, 2013.
Pistolesi, M., Cioni, R., Rosi, M., and Aguilera, E.: Lahar hazard assessment in the southern drainage system of Cotopaxi volcano, Ecuador: results from multiscale lahar simulations, Geomorphology, 207, 51–63, 2014.
Reiss, W.: Uber Lavastrome der Tungurahua und Cotopaxi, Zeitschr. Dt. Geol. Ges., 26, 907–927, 1874.
Reiss, W. and Stubel, A.: Das Hochgebirge der Republik Ecuador, ii: Petrographische Untersuchungen des Ostkordillere, Asher, Berlin, 1869–1902.
Ridolfi, F., Puerini, M., Renzulli, A., Menna, M., and Toulkeridis, T.: The magmatic feeding system of El Reventador volcano (Sub-Andean zone, Ecuador) constrained by texture, mineralogy and thermobarometry of the 2002 erupted products, J. Volcanol. Geoth. Res., 176, 94–106, 2008.
Robin, C., Samaniego, P., Le Pennec, J. L., Mothes, P., and Van Der Plicht, J.: Late Holocene phases of dome growth and Plinian activity at Guagua Pichincha volcano (Ecuador), J. Volcanol. Geoth. Res., 176, 7–15, 2008.

Rodolfo, K. S.: The Hazard from Lahars and Jökulhlaups, in: Encyclopedia of Volcanoes, edited by: Sigurdsson, Sigurdsson, H., Houghton, B., Rymer, H., Stix, J., and McNutt, S., Academic Press, 973–995, 1999.
Schmincke, H. U.: Volcanism, Springer, Berlin, 326 pp., 2004.
Scott, W. E., Nye, C. J., Waythomas, C. F., and Neal, C. A.: August 2008 eruption of Kasatochi volcano, Aleutian Islands, Alaska – resetting an island landscape, Arct. Antarct. Alp. Res., 42, 250–259, 2010.
Self, S.: The effects and consequences of very large explosive volcanic eruptions, Philos. T. Roy. Soc. A, 364, 2073–2097, 2006.
Self, S. and Rampino, M. R.: The relations between volcanic eruptions and climate change: still a conundrum, EOS T. Am. Geophys. Un., 69, 74–75, 85–86, 1988.
Sigurdsson, H. and Carey, S.: Volcanic disasters in Latin America and the 13th November 1985 eruption of Nevado del Ruiz volcano in Colombia, Disasters, 10, 205–216, 1986.
Smithsonian Institution: Volcano data, weekly and monthly reports, Global Volcanism Program, available at: http://volcano.si.edu/volcano.cfm?vn=352050 (last access: November 2015), 1999–2015.
Sodiro, L.: Relación Sobre la Erupción del Cotopaxi Acaecida el Día 26 de Junio, de 1877, Imprenta Nacional, Quito, 40 pp., 1877.
Steffke, A. M., Fee, D., Garces, M., and Harris, A.: Eruption chronologies, plume heights and eruption styles at Tungurahua Volcano: integrating remote sensing techniques and infrasound, J. Volcanol. Geoth. Res., 193, 143–160, 2010.
Stübel A.: Die Vulkanberge Ecuadors, Verlag des Museums für Volkerkunde, Leipzig, 1897.
Thouret, J. C.: Effects of the November 13, 1985 eruption on the snow pack and ice cap of Nevado del Ruiz volcano, Colombia, J. Volcanol. Geoth. Res., 41, 177–201, 1990.
Toulkeridis, T.: New, efficient educative prevention for Ecuador's volcano Cotopaxi, in: Cities On Volcanoes 4 (COV4), Quito, Ecuador, p. 142, 2006.
Toulkeridis, T.: The Summer 2006 Volcanic Crisis of Tungurahua, Ecuador: No Lessons Learned, in: AGU Spring Meeting Abstracts, 1, 02, 2007a.
Toulkeridis, T.: Volcanic crisis in Ecuador 1998–2007: Unprepared public versus unprepared authorities – some lessons learned, Japan 2, in: Cities On Volcanoes 4 (COV5), Shimabara, Japan, 116 pp., 2007b.
Toulkeridis, T.: Volcanic Hazard Preparedness in Ecuador, in: Cities On Volcanoes 6 (COV6), May–June 2010, Tenerife, España, p. 228, 2010.

Toulkeridis, T.: State of Volcanic Hazard Preparedness in Ecuador 2007–2012, in: Cities On Volcanoes 7 (COV7), Colima, Mexico, 2012.
Toulkeridis, T.: Volcanes Activos Ecuador, Santa Rita, Quito, Ecuador, 152 pp., 2013.
Toulkeridis, T. and Aguilera, E.: The avoidable disaster of Cotopaxi, Ecuador, in: Cities On Volcanoes 3 (COV3), Hawaii, USA, 134 pp., 2003.
Toulkeridis, T. and Aguilera, E.: The sum of all fears: Ecuador's Cotopaxi – Prevention versus Prediction, IAVCEI General assembly 2004, Pucón, Chile, 2004.
Toulkeridis, T. and Zach, I.: Wind directions of volcanic ash-charged clouds in Ecuador – implications for the public and flight safety, Geomat. Nat. Hazards Risks, in press, 2015.
Toulkeridis, T., Buchwaldt, R., and Addison, A.: When volcanoes threaten, Scientists Warn. Geotimes, 52, 36–39, 2007.
von Humboldt, A.: Geognostische und physikalische Beobachtungen über die Vulkane des Hochlandes von Quito, Erste Abhandlung, Ann. Phys. Chem., 40, 161–193, 1937.
von Humboldt, A.: Geognostische und physikalische Beobachtungen über die Vulkane des Hochlandes von Quito, Zweite Abhandlung, Ann. Phys. Chem., 44, 193–219, 1838.
von Humboldt, A.: Reise auf dem Río Magdalena, durch die Anden und Mexico, Teil 1, Akademie-Verlag, Berlin, 197 pp., 1986.
von Humboldt, A.: Briefe aus Amerika (1799–1804), Akademie-Verlag, Berlin, 176–179, 1993.
Whymper, E.: Travels Amongst the Great Andes of the Equator, Salt Lake City Peregrine Smith Books, 456 pp., 1892.
Wolf, T.: Memoria Sobre el Cotopaxi y su Ultima Erupción Acaecida el 26 de Junio de 1877, Imprenta de El Comercio, Guayaquil, 48 pp., 1878.
Wolf, T.: Crónica de los Fenómenos Volcánicos y Terremotos en el Ecuador, Quito, Imprenta de la Universidad Central, 167 pp., 1904.

Table 1. Summary of the chemical composition obtained from samples COT-1408-1, 2, 3 and 4.

Elements	COT-1408-1 norm. w.t. %	COT-1408-2 norm. w.t. %	COT-1408-3 norm. w.t. %	COT-1408-4 norm. w.t. %
Silicon	47 ± 2	43 ± 2	41 ± 2	42 ± 1
Sulfur	10 ± 1	14 ± 1	17 ± 1	24 ± 1
Calcium	13 ± 1	12 ± 1	12 ± 1	13 ± 1
Iron	17 ± 1	17 ± 1	17 ± 1	10 ± 1
Sodium	4.9 ± 0.3	6.3 ± 0.3	5.9 ± 0.3	4.6 ± 0.2
Potassium	2.1 ± 0.2	2.8 ± 0.2	2.2 ± 0.2	2.6 ± 0.2
Titanium	1.2 ± 0.1	1.8 ± 0.2	1.3 ± 0.2	1.9 ± 0.4
Magnesium	2.6 ± 0.4	2.0 ± 0.2	2.2 ± 0.3	1.2 ± 0.2
Manganese	1.3 ± 0.1	1.3 ± 0.1	1.3 ± 0.1	0.7 ± 0.1

Table 2. Summary of the size distributions obtained from samples COT-1408-1, 2, 3 and 4.

	Particles analyzed	Mean particle diameter (μm)	Standard deviation (μm)	Confidence interval (68 %) (μm)	Confidence interval (95 %) (μm)	Skewness
COT-1408-1	203	102.26	49.45	[98.8–105.7]	[95.4–109.3]	1.067
COT-1408-2	121	112.61	61.49	[107.0–118.2]	[101.5–123.7]	1.038
COT-1408-3	119	253.46	133.23	[241.3–265.7]	[229.3–277.6]	0.139
COT-1408-4	111	62.05	58.13	[51.1–72.9]	[56.5–67.6]	1.702

Table 3. Summary of the particle size distribution (see Fig. 10) from samples collected at the Lasso area on different days. Explanation see text.

Date	Location	# particles	Diameter (μm)	Standard deviation (μm)
22 Aug	Lasso Novacero	125	129.01	90.54
23 Aug	Lasso	168	90.54	52.46
25 Aug	Lasso Benefrut	187	93.47	55.47
25–26 Aug	Lasso-Pastocalle	123	67.02	39.42

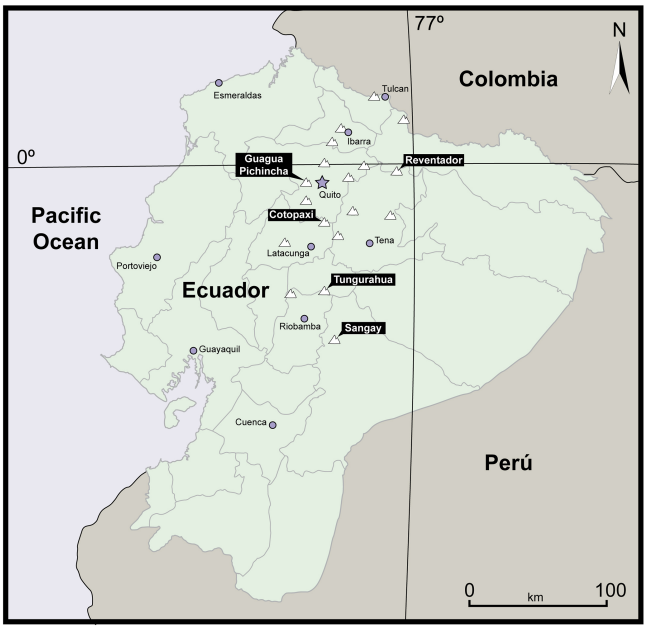

Figure 1. Ecuador's considered active volcanoes (white triangles) with the five volcanoes, which erupted the last 15 years generating ash clouds.

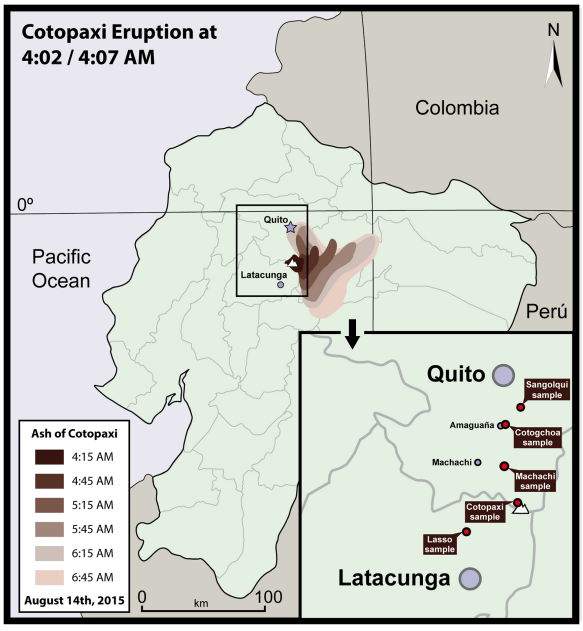

Figure 2. Ash cloud distribution of the 04:02 and 04:07 ECT events of the 14 August reactivation of Cotopaxi volcano. Distribution drawn based on images of the Ecuador Satellite Imagery of the Satellite Services Division of the National Environmental Satellite, Data, and Information Service (NESDIS). Inset in the bottom right shows the sample sites (see text for explanations).

Figure 3. Eruptive column of the 10:25 ECT event of the 14 August reactivation of Cotopaxi volcano. Photo courtesy by Fernando Iza.

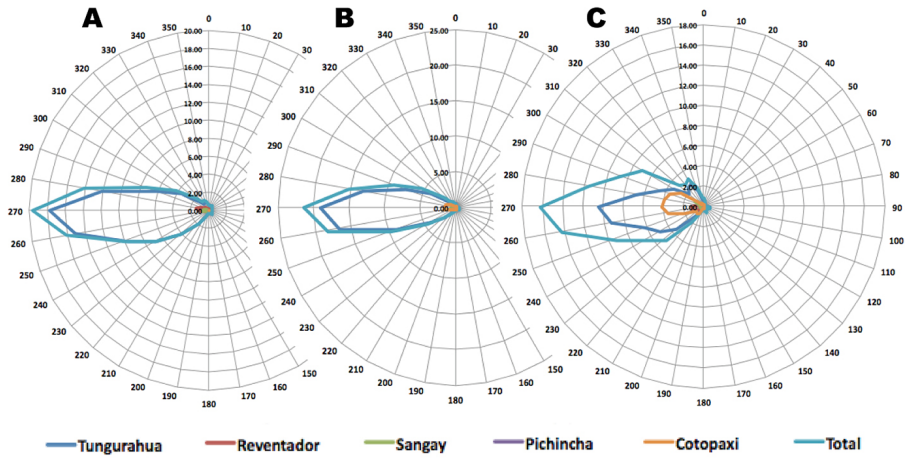

Figure 4. Wind directions of ash-charged clouds of five Ecuadorian volcanoes being active between September 1999 until September 2015 plotted in a rose-diagram, demonstrating the data of July, August and September, the time period of the reactivation of Cotopaxi volcano.

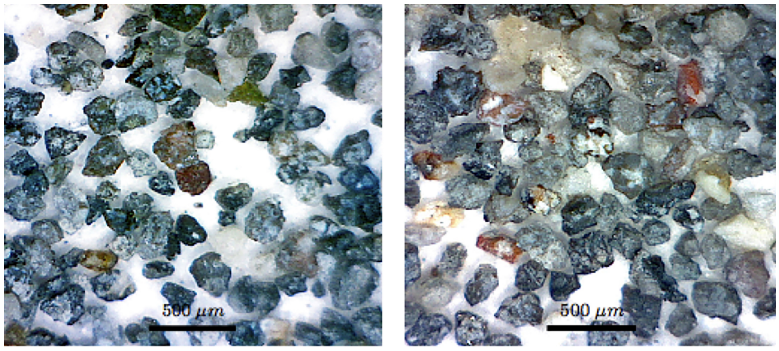

Figure 5. Optical microscope images of particles from sample COT-1408–3. Note the angular and sub-angular shapes of all minerals and rock fragments.

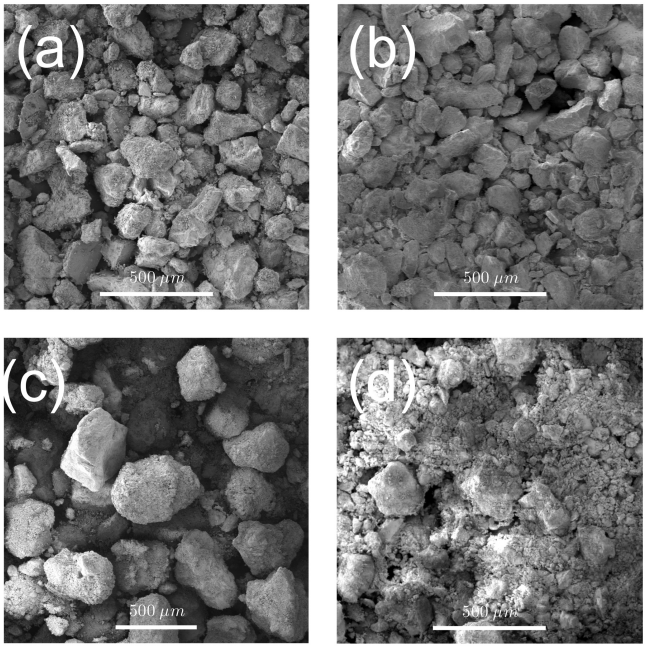

Figure 6. Typical SEM images obtained from **(a)**–**(d)** Samples COT-14-081, 2, 3 and 4 respectively. Note the fragmented, angular edges of all particles.

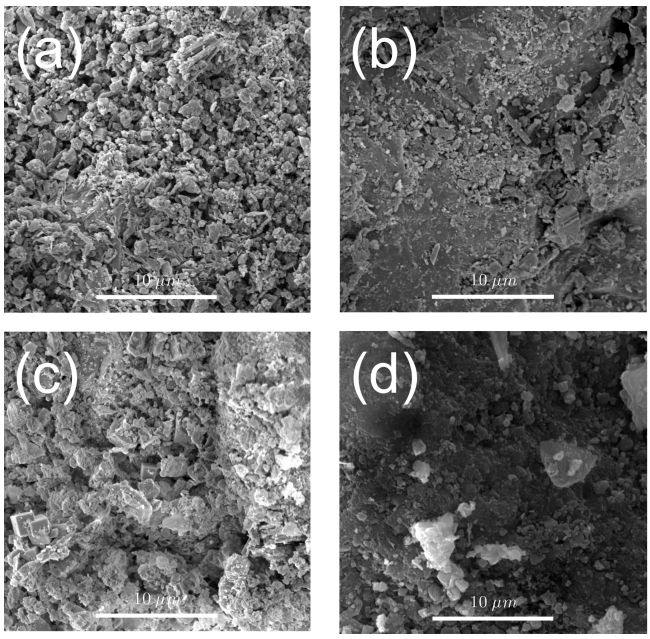

Figure 7. SEM micrographs (8000X) showing the surface structure of the particles corresponding to **(a)**–**(d)** samples COT-1408-1, 2, 3 and 4 respectively.

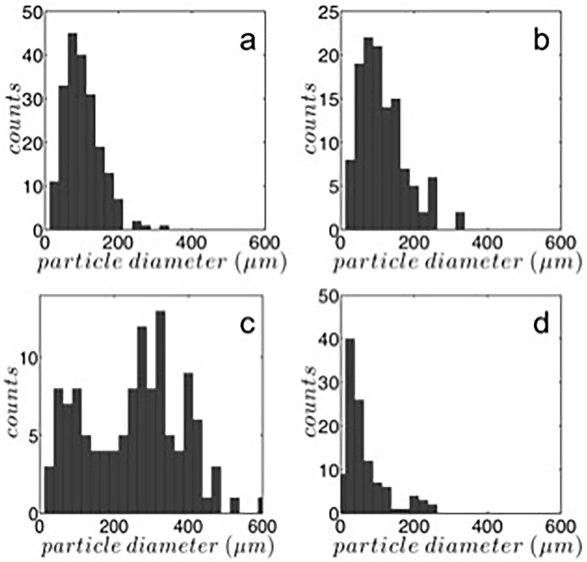

Figure 8. Particle diameter histograms obtained from **(a)**–**(d)** samples COT-1408-1, 2, 3 and 4. Note the finest-sized sample is naturally the one farthest to the crater.

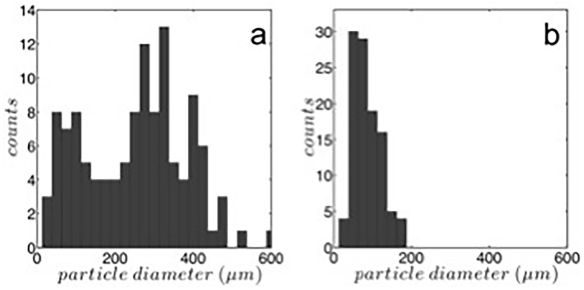

Figure 9. Grain-size distribution of Machachi samples collected on 14 and 23 August. Note that the particle size diminishes in time.

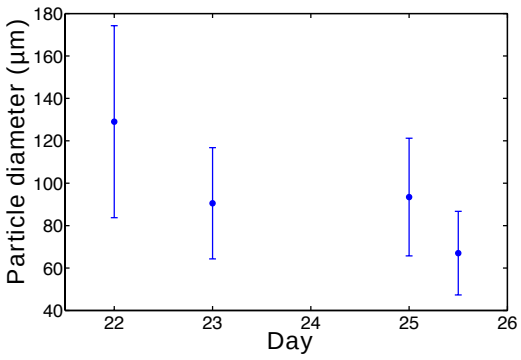

Figure 10. Evolution of the grain-size distribution of Lasso samples collected on 22, 23, 25 and during the night from 25 to 26 August. The origin of time axis corresponds to the 22 August. Note that the particle size diminishes in time.